AD-A239 791

SBI/NORDA

MENTATION PAGE

Form Approved OMB No. 0704-0188

Report Date. June 1991	3. Report Type and Dates Covered. Journal Article e040105

4. Title and Subtitle.
Similarities between various Lamb waves in submerged spherical shells, and Rayleigh waves in elastic spheres and flat half-spaces

5. Funding Numbers.
Program Element No. 61153N
Project No. 03202
Task No. 010
Accession No. DN255011

6. Author(s).
G. C. Gaunaurd* and M. F. Werby

7. Performing Organization Name(s) and Address(es).
Naval Oceanographic and Atmospheric Research Laboratory
Ocean Acoustics and Technology Directorate
Stennis Space Center, MS 39529-5004

8. Performing Organization Report Number.
JA 221:041:91

9. Sponsoring/Monitoring Agency Name(s) and Address(es).
Naval Oceanographic and Atmospheric Research Laboratory
Basic Research Management Office
Stennis Space Center, MS 39529-5004

10. Sponsoring/Monitoring Agency Report Number.
JA 221:041:91

11. Supplementary Notes.
*Naval Surface Warfare Center Research Department
J. Acoust. Soc. Am

DTIC ELECTE AUG 23 1991 S D

12a. Distribution/Availability Statement.
Approved for public release; distribution is unlimited.

12b. Distribution Code.

13. Abstract *(Maximum 200 words).*

A variety of resonance features are studied in the back-scattering cross sections (BSCS) of an air-filled metal spherical shell submerged in water and insonified by a plane cw sound wave. Rayleigh (R) and whispering gallery (WG) waves were originally investigated for vibrational purposes for (flat) half-spaces in contact with vacuum. Lamb waves were originally studied in flat plates also in contact with vacuum. These old findings are generalized to the cases of an elastic spherical shell (o.d./i.d. = 2a/2b) fluid-loaded on both surfaces, and excited by an incident plane wave. The various (leaky-type) Lamb waves present in the shell are shown to reduce to the earlier R/WG waves as $a \gg 1 \gg b$ and $\rho_f \to 0$. The manner in which each one of these various shell waves manifests itself in the various frequency bands of the shell's BSCS as perceived by a remote sensor is also studied. Dispersion plots for the various phase velocities of the various waves are displayed in very wide (i.e., $0<ka<500$) bands, and a number of analogies between Lamb and R/WG waves are obtained as the submerged shell becomes a solid sphere ($b \ll a$), and vice versa ($b \lesssim a$). The fluid loadings, the finite shell thickness, and the curvatures of the structure all generate novel types of waves in the shell (that manifest their effects in its BSCS) that could have never emerged from earlier models that ignored these effects, and which are analyzed here.

91-08709

14. Subject Terms.
Acoustic scattering, shallow water, waveguides

15. Number of Pages.
9

16. Price Code.

17. Security Classification of Report.	18. Security Classification of This Page.	19. Security Classification of Abstract.	20. Limitation of Abstract.
Unclassified	Unclassified	Unclassified	SAR

NSN 7540-01-280-5500

Standard Form 298 (Rev. 2-89)
Prescribed by ANSI Std. 239-18
298-102

91 8 22 048

Similarities between various Lamb waves in submerged spherical shells, and Rayleigh waves in elastic spheres and flat half-spaces

G. C. Gaunaurd
Naval Surface Warfare Center Research Department (R42), White Oak, Silver Spring, Maryland 20903-5000

M. F. Werby
Naval Ocean and Atmospheric Research Laboratory (221), Numerical Modelling Division, Bay St. Louis, Mississippi 39524

(Received 31 August 1990; accepted for publication 12 February 1991)

A variety of resonance features are studied in the back-scattering cross sections (BSCS) of an air-filled metal spherical shell submerged in water and insonified by a plane cw sound wave. Rayleigh (R) and whispering gallery (WG) waves were originally investigated for vibrational purposes for (flat) half-spaces in contact with vacuum. Lamb waves were originally studied in flat plates also in contact with vacuum. These old findings are generalized to the cases of an elastic spherical shell (o.d./i.d. $= 2a/2b$) fluid-loaded on both surfaces, and excited by an incident plane wave. The various (leaky-type) Lamb waves present in the shell are shown to reduce to the earlier R/WG waves as $a \gg 1 \gg b$ and $\rho_f \to 0$. The manner in which each one of these various shell waves manifests itself in the various frequency bands of the shell's BSCS as perceived by a remote sensor is also studied. Dispersion plots for the various phase velocities of the various waves are displayed in very wide (i.e., $0 < ka < 500$) bands, and a number of analogies between Lamb and R/WG waves are obtained as the submerged shell becomes a solid sphere ($b \ll a$), and vice versa ($b \lesssim a$). The fluid loadings, the finite shell thickness, and the curvatures of the structure all generate novel types of waves in the shell (that manifest their effects in its BSCS) that could have never emerged from earlier models that ignored these effects, and which are analyzed here.

PACS numbers: 43.35.Mr, 43.40.Ey

INTRODUCTION

Strictly speaking, Rayleigh waves propagate along the surface of (semiinfinite) half-spaces in contact with vacuum. In practice, however, there are no elastic half-spaces. So, one may ask if Rayleigh waves can exist on the (flat) surface of a layer of possibly infinite extent, but of finite thickness. Numerous authors have studied and answered this question,[1-7] which by now is summarized in various monographs.[8-15] Briefly, for thick layers — those with thickness d greater than the Rayleigh wavelength λ_R — only two ordinary Lamb waves (viz., A_0 and S_0) are essentially excited in the plate. For $d > \lambda_R$, the propagation characteristics of these two Lamb modes are very similar to those of a Rayleigh wave. Thus the answer to the above question has been given in the affirmative.

Lamb wave propagation in a fluid-loaded (flat) plate has also received much attention. Again, various reviews and monographs have summarized this situation,[15-20] which include numerous references. In this case, the wave numbers (and modes) are determined from a set of coupled characteristic equations that yield the eigenfrequencies (and eigenfunctions), now accounting for the fluid loading.

When the structure is now a shell or a solid-curved elastic body, the analysis of the corresponding Lamb or Rayleigh waves on these curved objects has received less study,[21-23] but some general foundations involving curvature[22-23] and fluid loading[24] have been established. It is the purpose of the present work to further extend this foundation and examine basic theoretical similarities between the (generalized) Rayleigh and Lamb waves in convex solid elastic bodies and elastic shells, respectively, particularly when these bodies are subject to the influence of fluid loading.

I. THEORETICAL BACKGROUND

A plane sound wave travels through a fluid medium and impinges on a thin elastic, air-filled, spherical shell of outer (or inner) radii a (or b). Its (normalized) backscattering cross section is given by[21]

$$\frac{\sigma}{\pi a^2} = |f_\infty(\pi,x)| = \left|\sum_n{}' f_n(\pi,x)\right|^2 = \left|\frac{2}{ix}\sum_n{}' (-1)^n(2n+1)A_n(x)\right|^2, \quad (1)$$

where $f_\infty(\pi,x)$ is the form function in the backscattering direction, $\theta = \pi$. We define a nondimensional frequency $x = k_1 a$, where $k_1 = \omega/c_1$. The circular frequency is ω and c_1 is the sound speed in the outer fluid (i.e., medium No. 1, water). The coefficients $A_n(x)$ are determined from the (six) boundary conditions at the interfaces $r = a,b$ as ratios of two 6×6 determinants, viz.,

$$A_n(x) = -B_n/D_n$$

$$= \frac{-1}{D_n}\begin{vmatrix} \mathrm{Reg}\, d_{11} & d_{12} & d_{13} & d_{14} & d_{15} & 0 \\ \mathrm{Reg}\, d_{21} & d_{22} & d_{23} & d_{24} & d_{25} & 0 \\ 0 & d_{32} & d_{33} & d_{34} & d_{35} & 0 \\ 0 & d_{42} & d_{43} & d_{44} & d_{45} & d_{46} \\ 0 & d_{52} & d_{53} & d_{54} & d_{55} & d_{56} \\ 0 & d_{62} & d_{63} & d_{64} & d_{65} & 0 \end{vmatrix}, \tag{2}$$

where

$$D_n(x) = \begin{vmatrix} d_{11} & d_{12} & d_{13} & d_{14} & d_{15} & 0 \\ d_{21} & d_{22} & d_{23} & d_{24} & d_{25} & 0 \\ 0 & d_{32} & d_{33} & d_{34} & d_{35} & 0 \\ 0 & d_{42} & d_{43} & d_{44} & d_{45} & d_{46} \\ 0 & d_{52} & d_{53} & d_{54} & d_{55} & d_{56} \\ 0 & d_{62} & d_{63} & d_{64} & d_{65} & 0 \end{vmatrix}. \tag{3}$$

The 28 (nonvanishing) elements, d_{ij} have been listed elsewhere.[21] All the elements depend on x, on $x_{d2} = \omega/c_{d2}$, on $x_{s2} = \omega/c_{s2}$, and on $x_3 = \omega/c_3$, where c_{d2} (c_{s2}) is the dilatational (or shear) wave speed in the shell, and c_3 is the sound speed in the inner fluid. Since $x_{d2} = (c_1/c_{d2})x$, $x_{s2} = (c_1/c_{s2})x$, and $x_3 = (c_1/c_3)x$, all the elements ultimately depend on x, and so do coefficients $A_n(x)$. This formulation is exact since the shell motions are described by the three-dimensional equations of elastodynamics. This solution has been programmed for numerical evaluation.

Subtraction of the (rigid) modal backgrounds usually isolates the pure resonances in the typical manner of the resonance scattering theory (RST).[23] These backgrounds have coefficients of the form

$$A_n^{(r)}(x) = -j_n'(x)/h_n^{(1)\prime}(x). \tag{4}$$

The sum of those (residual) modal resonances is then

$$\begin{aligned} |f_\infty^{(\mathrm{res})}(\pi,x)| &= \left| \sum_{n=0}^{\infty} f_n^{(\mathrm{res})}(\pi,x) \right| \\ &= \left| \sum_{n=0}^{\infty} [f_n(\pi,x) - f_n^{(r)}(\pi,x)] \right| \\ &= \left| \frac{2}{ix} \sum_{n=0}^{\infty}{}' (-1)^n (2n+1) \right. \\ &\quad \left. \times [A_n(x) - A_n^{(r)}(x)] \right|, \end{aligned} \tag{5}$$

which we have often called the residual or resonance response. We have shown[25] that the partial waves, $|f_n(\pi,x)|$ contained within the sum in Eq. (1) can be *exactly* decomposed in the form

$$|f_n(\pi,x)| = \left| \frac{2n+1}{x} e^{2i\xi_n^{(r)}} \left(2ie^{-i\xi_n^{(r)}} \sin \xi_n^{(r)} + \sum_l \frac{z_1^{-1} - z_2^{-1}}{F_n^{-1} - \mathrm{Re}\, z_1^{-1} - i\,\mathrm{Im}\, z_1^{-1}} \right) \right|, \tag{6}$$

where F_n^{-1} is proportional to the shell's mechanical impedance, and z_i^{-1} ($i = 1,2$) are proportional to its acoustic impedances, as defined elsewhere.[25] These exact expressions represent contributions from the background associated with reflection from an impenetrable body (first term) and from the structural resonances that cause reradiation (second term). These expressions can be further *linearized* in the current (approximate) way of the RST, that will not be further shown here. Equation (6) serves merely to point out that complex eigenfrequencies x_{nl}, are obtained from the vanishing of the entire (complex) denominator shown in the fraction term (viz., $F_n^{-1} = z_1^{-1}$), while the (real) resonances in this "rigid-background" case, are roots of the *real* part of the denominator (viz., $F_n^{-1} = \mathrm{Re}\, z_1^{-1}$). These conditions for complex eigenfrequencies and real resonances are equivalent to the vanishing of the denominator determinant in Eq. (3) [viz., $D_n(x) = 0$], or of its regular part in Eq. (2) [viz., $B_n(x) = \mathrm{Reg}\, D_n(x) = 0$], respectively. Once the (complex) zeros of $D_n(x)$ are found, say x_{nl}, then the phase velocities of the various types of Lamb waves present in the shell (and their attenuations) can be obtained from the expressions

$$\frac{c_l^p(x)}{c_1} = \frac{\mathrm{Re}\, x_{nl}}{n+\frac{1}{2}}, \quad \theta_l^p(x) = \frac{1}{\mathrm{Im}\, x_{nl}}, \tag{7}$$

for each value of the index pair (n,l). We have developed numerical programs to determine the zeros of these determinants, and to calculate the corresponding phase velocities and attenuations of the surface waves associated with these zeros. We have also noted that [23] the phase velocities and attenuations of the (Lamb) surface waves of a spherical shell *in vacuo* are found by means of Eq. (7) from the zeros of a simpler determinant of order 4×4 rather than 6×6, given by

$$D_{56}^{21}(x) = \begin{vmatrix} d_{12} & d_{13} & d_{14} & d_{15} \\ d_{32} & d_{33} & d_{34} & d_{35} \\ d_{42} & d_{43} & d_{44} & d_{45} \\ d_{62} & d_{63} & d_{64} & d_{65} \end{vmatrix}, \tag{8}$$

which exactly accounts for the shell's double curvature and elastic composition, but ignores the presence of the fluid loading on its two surfaces.

Finally, it should be noted that the Rayleigh-wave velocity in a flat half-space, where it was originally introduced,[1,8] comes out to be the real root of a fourth-order algebraic equation, which can be approximated by the simple relation[8]

$$C_R \cong [(0.87 + 1.12\nu)/(1+\nu)]c_s, \tag{9}$$

where ν is Poisson's ratio and c_s is the shear speed. This is an analytic approximation quoted by Viktorov[8] of an earlier numerical evaluation of the Rayleigh speed for a flat, elastic, half-space in contact with vacuum. The numerical evaluation was originally found by Knopoff,[26] and it was later reported in textbooks (viz., Ref. 11, p. 34). For a spherical shell of radii a, b, there is no true Rayleigh speed since now one has (spherically modified) Lamb modes and surface waves. However, in the limit $b \to 0$ (i.e., for a solid elastic sphere), a "corresponding" Rayleigh speed is obtained which is slightly higher than that predicted by Eq. (9) for the flat interface. In fact, all the spherical Lamb branches, $A_1, S_1, \ldots, A_n, S_n$ of the dispersion curves associated with all the Lamb surface waves for the shell also approach their own

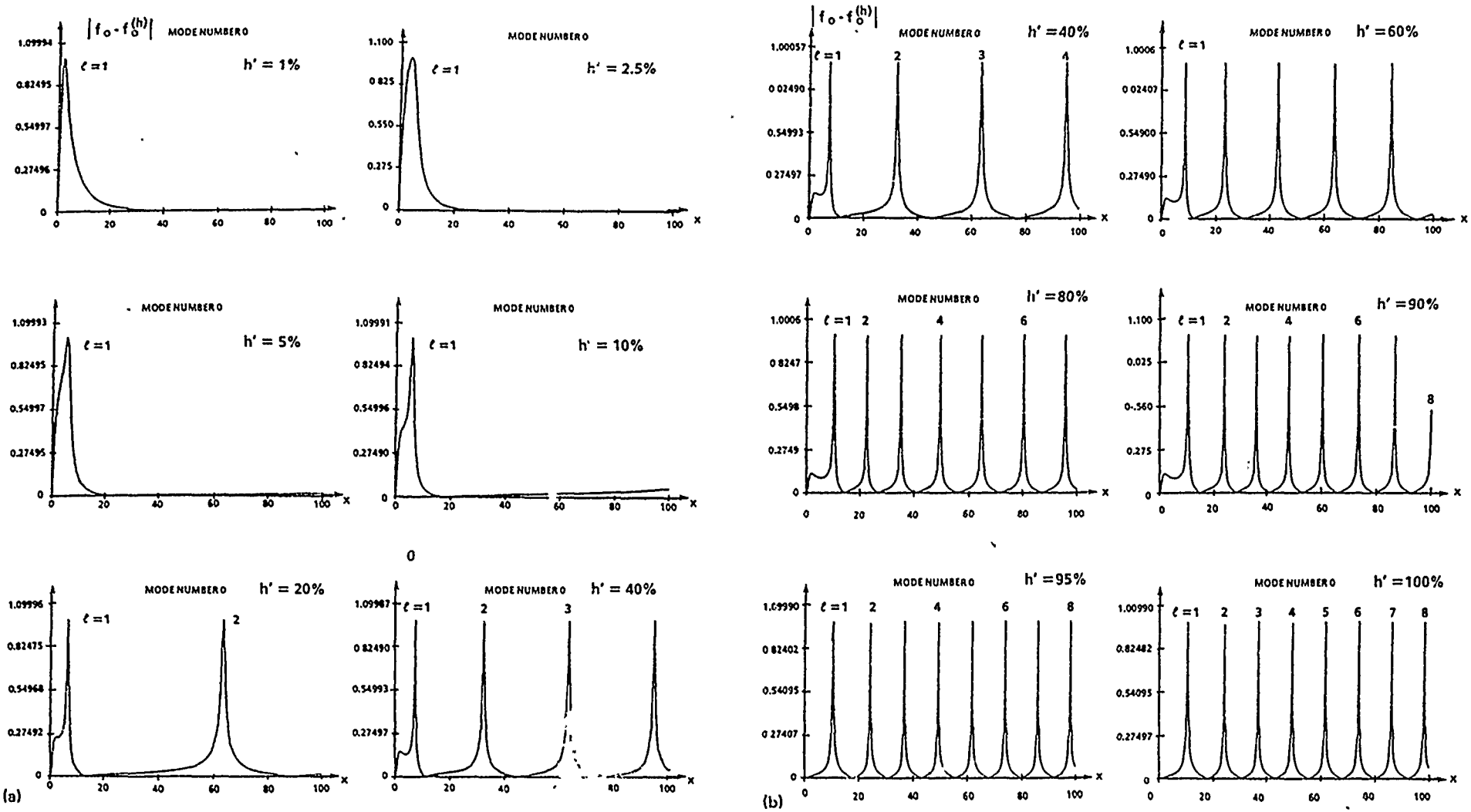

FIG. 1. Isolated resonances (or residual responses) contained within the zeroeth (i.e., A_0) Lamb mode of a fluid-loaded steel spherical shell of increasing (relative) thickness. (a) $h' = 1\%$, 2.5%, 5%, 10%, 20%, and 40%; (b) $h' = 60\%$, 80%, 90%, 95%, and 100% (solid sphere case). The modal resonances are labeled in each case by the index l.

Rayleigh speed in the limit of a solid elastic sphere (i.e., for $b \to 0$ or $h' = 100\%$). So, the Rayleigh speed in these cases is mode-order (i.e., n) dependent. Ultimately, for high-order modes, which is a situation equivalent to high frequencies or to large values of a, the value of c_R for a flat interface, given by Eq. (9), is then reached.

II. NUMERICAL RESULTS

Figure 1(a) and (b) shows the residual or resonance response associated with the $n = 0$ elastic mode of an air-filled steel spherical shell of variable thickness immersed in water. This display of residual responses is obtained by the suppression of suitable (rigid) modal backgrounds. The relative shell thickness $h' \equiv h/a = (a - b)/a$ ranges in value from 1% to 100% in 11 stages. These are: $h' = 1\%$, 2.5%, 5%, 10%, 20%, 40%, 60%, 80%, 90%, 95%, and 100%. The last stage corresponds to a solid steel sphere in water. All the calculations are displayed in the broad (nondimensional) frequency band: $0 \leqslant x \equiv k_1 a \leqslant 100$. The $n = 0$ mode and its associated residual response, after background suppression, is the one usually related to purely dilatational features. Table I lists all the required material parameters for the shell and the fluids that load it on its two surfaces. Simple observation of these plots shows that thin shells support fewer modes and isolated resonance features than thicker ones. Up to thicknesses of about 20% only one or two resonance features (i.e., the $l = 1$ and/or 2) are visible in the resulting graphs within the displayed band. For thicker shells more features appear until about $l = 8$ resonances are seen at thicknesses of 90%, 95% and 100%. The first one of these resonances features (i.e., the $l = 1$) would be the analog of the Rayleigh resonance for a *solid* sphere, while all the others would "correspond" to the whispering gallery resonance features ($l \geqslant 2$). However, here we have a *shell* in which the $l = 1$ feature, present in all the modes, is due to the first antisymmetric (flexural) *shell* Lamb wave A_0. This is the spherical counterpart of the $\overline{A}_0$ surface wave that has been the subject of many studies[1-7] for the case of flat *plates*. Hence, our A_0 is a spherical Lamb wave that generalizes the $\overline{A}_0$ Lamb wave of plates. This flexural shell wave "corresponds" to the Rayleigh wave for solid elastic spheres (viz., $b \to 0^+$) and also ultimately, to the Rayleigh wave in flat elastic half-spaces ($a \gg 1$).

It should be pointed out that for an air-filled shell, the effect of the air-borne reverberations will manifest itself as a series of very narrow resonance spikes in the BSCS, or in the isolated residual responses of Fig. 1. These skinny resonances are several *thousand* times narrower than the ones shown in Fig. 1. They look like a "noise effect," and are easily missed if high-resolutions are not used in the generation of the plots. We have intentionally suppressed them here, since they do not add to the points of present concern.

Figure 2 displays the dispersion plots for the phase velocities of this (generalized) A_0 (Lamb) wave in the spherical shell as a function of $x(\equiv k_1 a)$ for eight shell thicknesses. These thicknesses are: $h' = h/a = 10\%$, 20%, 40%, 80%, 90%, 95%, and 100% (solid). For thicknesses below 40% the dispersion curves exhibit an upward turn due to the (double) curvature of the shell, in contrast to those observed in earlier works which were based on plate theories or approaches to generate the corresponding dispersion plots.

Figure 3 exhibits the value of the phase velocities of each shell mode ranging from $n = 2$ to 7, as a function of the relative thickness, h', in an appropriate range (viz., $10\% \leqslant h' \leqslant 100\%$). These shell modes $n = 2,3,...7$, respectively, correspond to the Lamb modes usually labeled A_1, S_1, A_2, S_2, A_3, and S_3. As seen in Fig. 3, for $h' = 100\%$, the phase velocity c'' of all the modes takes on a value near 3.5 km/s, that decreases with increasing mode order. Higher order modes such as $n = 30$—which would correspond to the A_{15} Lamb wave—exhibit lower values of the phase velocity in the solid sphere limit (i.e., for $h' = 100\%$). The value in that case is $c'' = 3.14$ km/s (cf. Fig. 4, bottom plot). Such value is reached at a shell thickness of $h' \cong 40\%$, and it remains constant from $h' \cong 40\%$ up to 100%. The value of the Rayleigh speed for a flat elastic half-space, c_R, as approximately given by Eq. (9), turns out to be $c_R \cong 3.00$ km/s using the values of the material parameters listed in Table I. This is the limiting value for all modes at sufficiently large values of a, or for sufficiently high frequencies. To further examine some of these points, we generate the usual type of dispersion plot for the phase velocity of the single Lamb wave A_0 vs x, for various thicknesses such as: $h' = 1\%$, 2.5%, 5%, 10%, and 20%. The result is displayed in Fig. 5. The way such a plot is generated is by solving for the roots, x_{nl} of $D_n(x) = 0$, using a complex rootfinder, and then substituting those roots into the first of Eqs. (7). All the dispersion curves exhibit an upward turn at low frequencies. At higher frequencies, they all approach the Rayleigh speed, c_R, found above. This high-$k_1 a$ limit is approached faster the thicker the shell becomes. The curves are drawn solid above the value of the sound speed in the outer water (viz., $c_1 \simeq 1.5$ km/s), and dashed below it. This mode A_0 is only excited above the value of c_1. For frequencies x such that $c'' < c_1$, this mode is not present in the shell. Other, water-borne waves exist in this "subsonic" region. We note that the frequency at which $c'' = c_1$ is Cramer's *coincidence frequency*[13] at which strong flexural vibrations are excited in the shell, which are then communicated to its backscattering cross section.[21]

TABLE I. Material parameters of the shell and the fluids.

	Density ρ(g/cm^3)	Dilatational c_d(cm/s)	Shear speed c (cm/s)	Young's modulus E(dyn/cm^2)	Poisson's ratio ν
Stainless steel	7.7	5.95×10^5	3.24×10^5	20.8×10^{11}	0.289
Water	1.0	1.4825×10^5	0	...	...
Air	0.0012	0.344×10^5	0	...	...

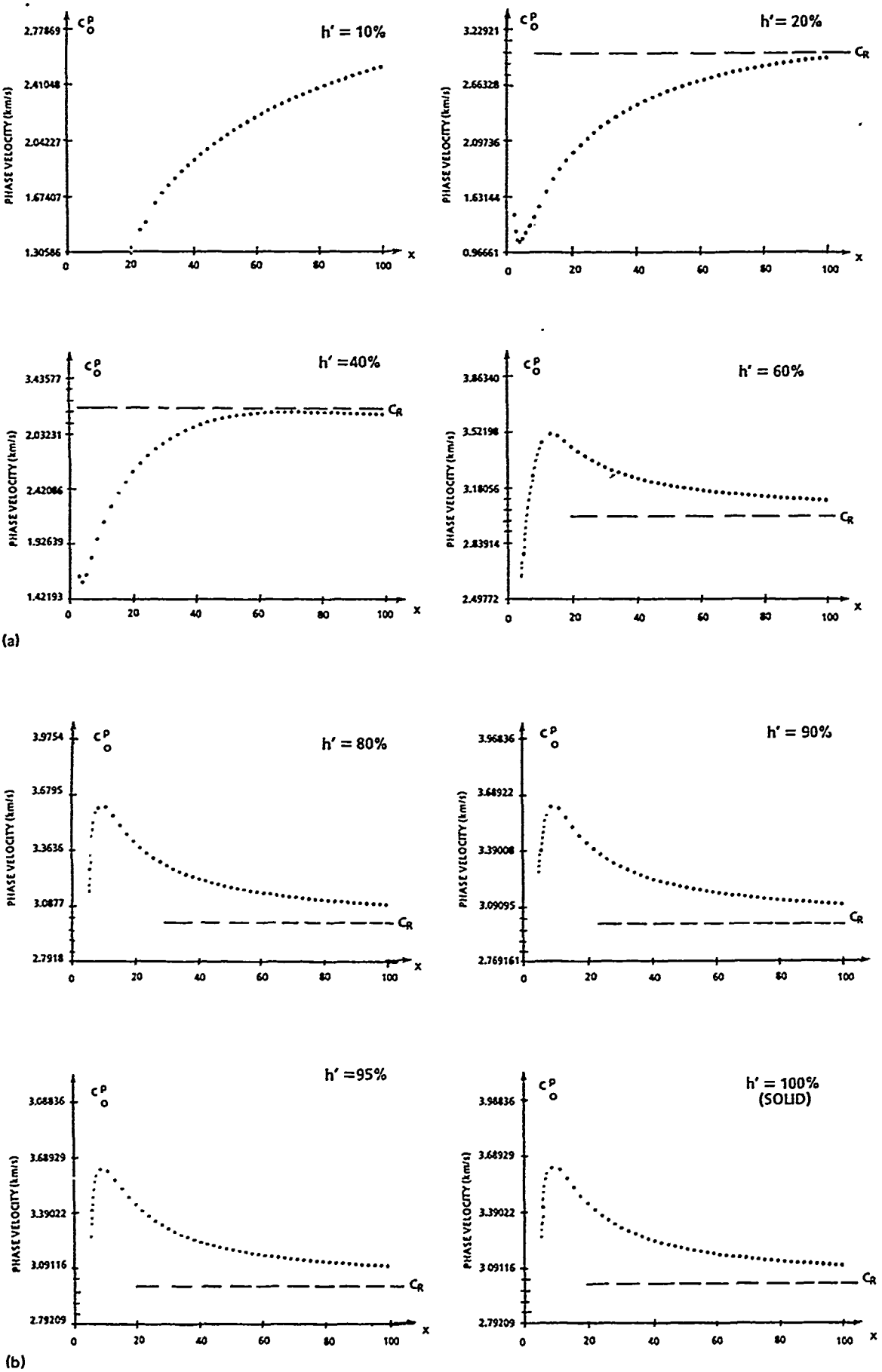

FIG. 2. Dispersion plots for the phase velocity c_n^p of the A_n Lamb wave in the band $0 \lesssim x = k_1 a \lesssim 100$, for a spherical steel shell in water of increasing (relative) thickness [viz., (a) $h' = 10\%, 20\%, 40\%, 60\%$, (b) $h' = 80\%, 90\%, 95\%$, and 100% (solid sphere)]. The limit of c_R—as given by Eq. (9)—seems to be approached in all cases for x large.

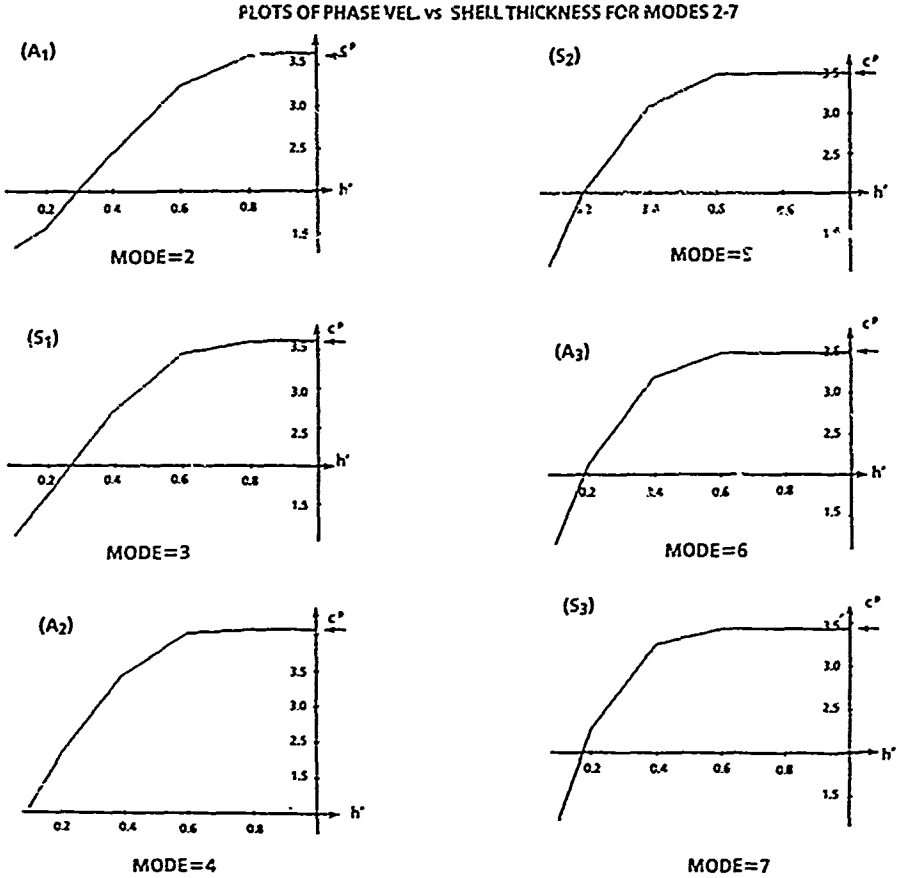

FIG. 3. The phase velocity of various shell modes (viz., A_1, S_1, A_2, S_2,....) as function of shell (relative) thickness $h' \equiv h/a$. The c^p units are km/s. All modes tend to a value near 3.5 km/s, in the solid sphere ($h' = 1$) limit.

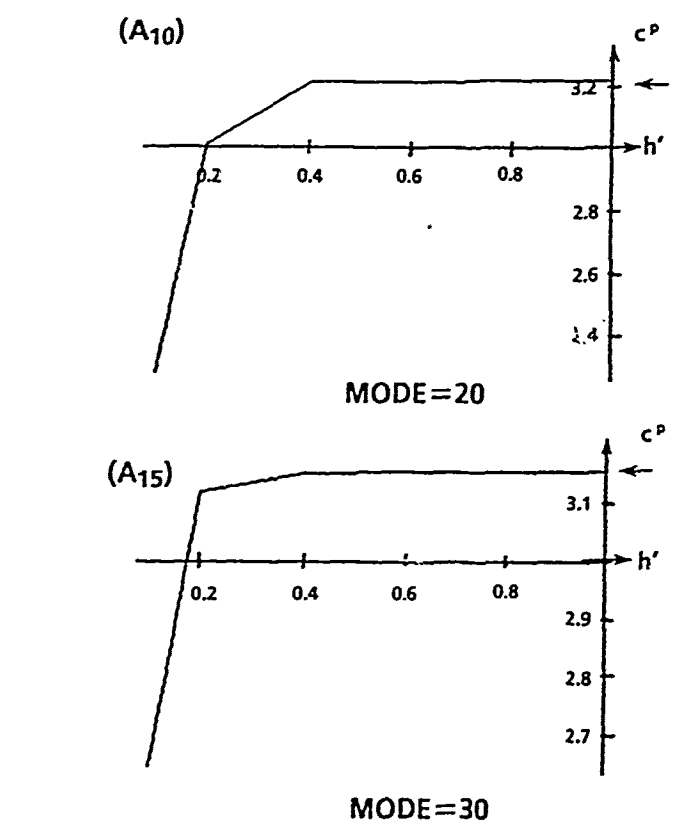

FIG. 4. Analogous to Fig. 3 but for higher-order modes, as high as A_{15}. The limit value for $h' = 1$ takes on a lower value of 3.14 km/s. This value is already reached at a shell thickness of $h' = 40\%$.

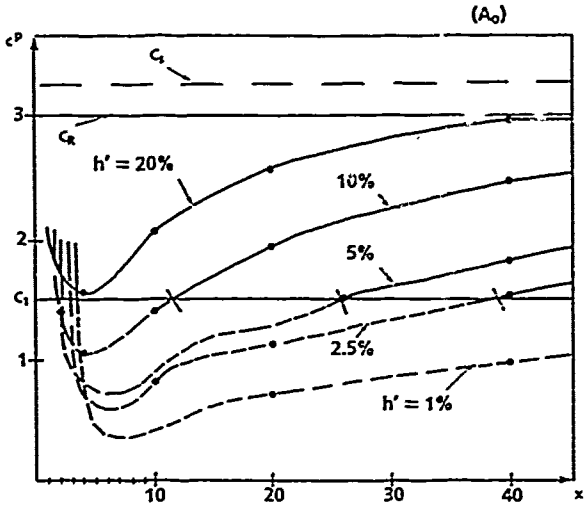

FIG. 5. Dispersion plots of the phase velocity c^p (km/s) of the A_0 Lamb wave vs x, for a steel spherical shell in water of increasing thickness (viz., $h' \equiv 1\%, 2.5\%, 5\%, 10\%$, and 20%). The frequencies at which the curves cross the present value of c_1 ($\equiv 1.4825$ km/s) is the "coincidence" frequency x_c. Mode A_0 exists only for $x > x_c$. For all thicknesses, the curves approach c_R for $x \gg 1$. At low frequencies all curves exhibit an upward bend, due to the shell (double) curvature.

Below coincidence, another shell mode is always present, namely the S_0 mode. The dispersion curves for the phase velocities of this Lamb wave, S_0, are displayed in Fig. 6 for the same shell thicknesses used in Fig. 5. All the curves approach c_s from above, as ($k_1 a \equiv$) x increases to large values. The thicker the shell the faster the dispersion curve will approach the c_s limit. At the low-frequency end, all the curves exhibit an upward bend to high values due to the shell's (double) curvature. This mode is always "on," above and

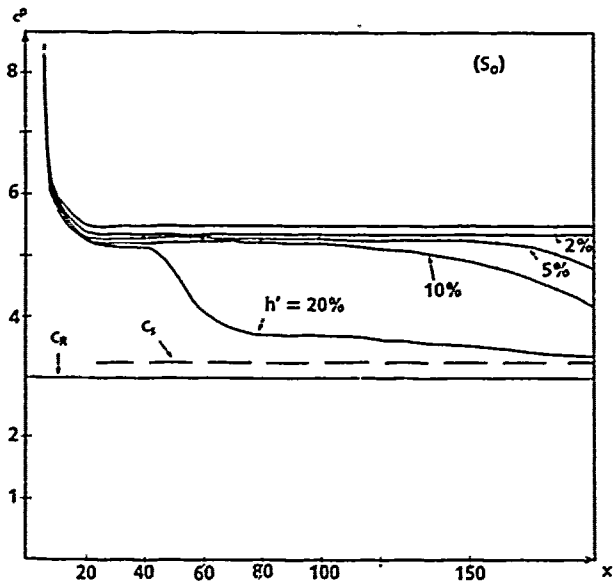

FIG. 6. Dispersion plots of the phase velocity c^p (km/s) of the S_0 Lamb mode/wave vs x. This is for a steel spherical shell in water of increasing thickness ($h' = 1\%, 2.5\%, 5\%, 10\%, 20\%$). The displayed band is $0 < x \equiv k_1 a < 190$. All the curves seem to approach the value of c_s as $x \gg 1$. This Lamb mode, S_0, exists above and *below* the coincidence frequency, x_c.

below the coincidence frequency. As we have seen before, in the band: $0 < x < 100$ the two predominant modes are A_0 and S_0. This is made evident in the lower part of Fig. 7, which was constructed for a spherical steel shell of $h' \equiv 5\%$. At higher frequencies (i.e., $x > 100$), other modes start to enter the picture, as we display in the upper part of Fig. 7. For this thickness, modes A_1, S_1, and S_2 already enter the picture, in addition to A_0 and S_0 in the broad band: $0 < x < 500$. For either broader bands or thicker shells, more of these Lamb modes/waves will produce a contribution. The construction of Fig. 7 follows the same pattern outlined for Figs. 5 and 6.

The numbers along the various branches of Fig. 7 correspond to values of the modal order n, obtained from a partial-wave expansion of the residual responses $|f_n(x) - f_n^{(\text{rig})}(x)|$ for higher values of n, similar to those displayed in Fig. 1 for the mode-order $n = 0$. Further details will be given elsewhere, particularly the *connection* between (generalized) Lamb poles for a shell, and Rayleigh poles for an elastic sphere in water. These later ones have already received some attention.[27]

We close by emphasizing the obvious point that the findings obtained above for the phase velocities of the various categorized types of surface waves considered here, and for their transition from one type to another as the shell-size grows, have emerged from an analysis of the BSCSs (or the residual responses) of the shell immersed in an acoustic medium. This is the only type of information available to a remotely sensing sonar. The large volume of works on elastic surface and bulk waves[8-12] usually pertains to the vibratory responses of (these) flat surfaces *in vacuo*, without any connection to acoustical scattering situations. The present results are not only novel from the purely vibratory point of view of fluid-loaded shells, but they are all extracted from the intricate pattern of "wiggles" present in the remotely sensed cross sections.

III. CONCLUSIONS

The first (i.e., $l = 1$) antisymmetric flexural Lamb resonance (or leaky surface wave) present in the modes of a steel spherical shell in water is the analog of the (generalized) Rayleigh resonance (or leaky surface wave) in a submerged elastic steel sphere. To prove this point we showed the modal resonances present in the residual responses (cf. Fig. 1) of the $n = 0$ mode of an elastic shell of increasing thickness that ultimately becomes a solid sphere. The dispersion plots for the phase velocity of the spherical, flexural, A_0 Lamb wave were then calculated and displayed for increasing shell thickness (cf. Fig. 2) showing that in the large-x limit these curves approach the flat half-space Rayleigh speed, c_R. We further investigated the phase-velocity variations of a number of higher order modes ($n = 2,3,\ldots,30$) as a function of (relative) shell thickness h'. In the solid sphere limit (i.e., $h' \to 100\%$, or $b \to 0$), the phase velocity c^p of each mode seems to approach the value of the Rayleigh speed for that spherical mode. For higher-order modes (or for larger x values), the value of the Rayleigh wave speed, c_R, for a flat interface is then eventually reached. Figure 4 shows that for the A_{15} mode this value seems to be quite close to the value already reached by a shell thickness of about $h' = 40\%$.

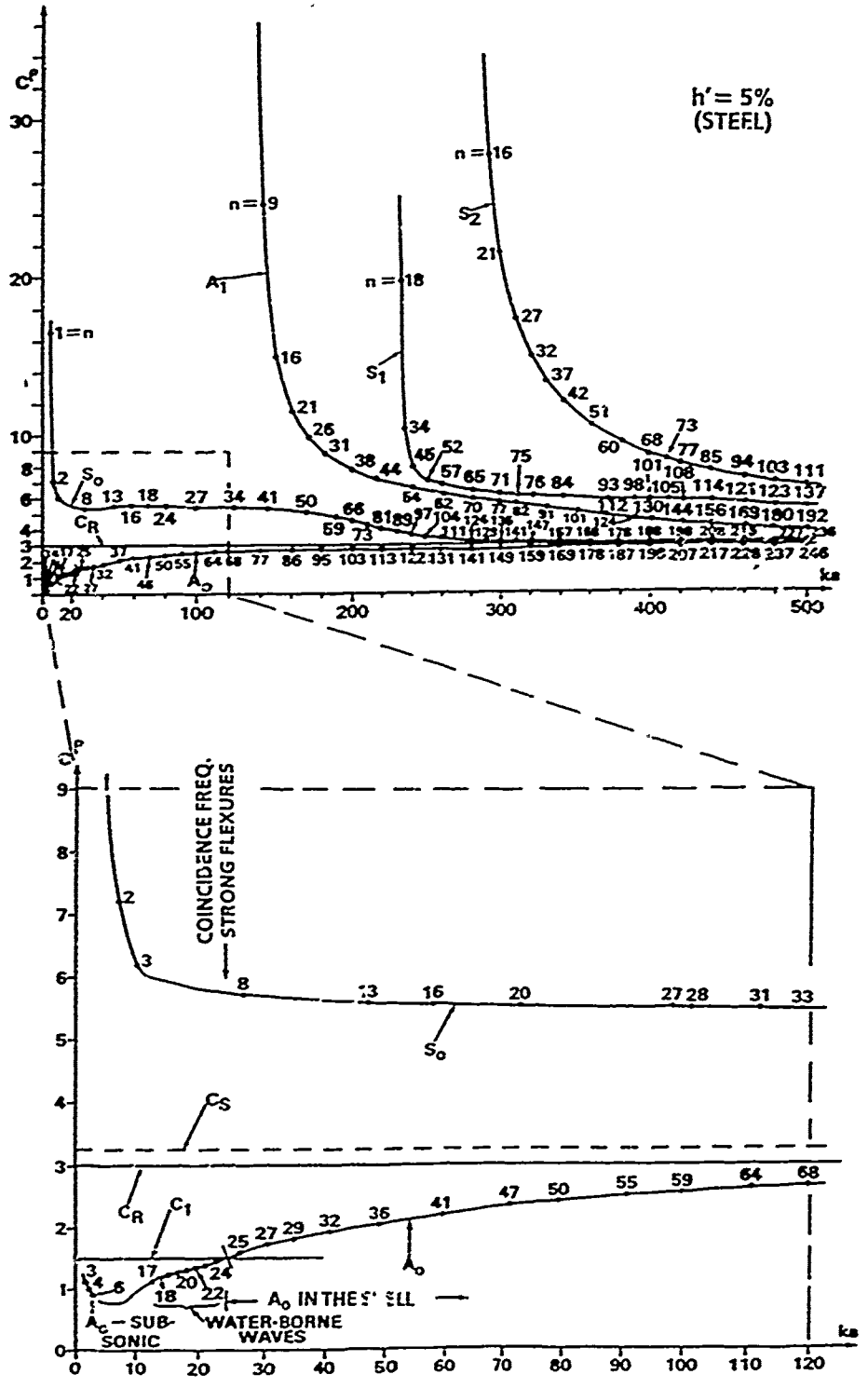

FIG. 7. This is a display of the dispersion curves for the phase velocities, c^p, of the various Lamb modes/waves A_n, S_n, A_1, S_1, S_2,..., present in a steel spherical shell in water of fixed thickness (viz., $h' = 5\%$), as the frequency is varied in a broader band (viz., $0<x<500$, top). The lower graph is a detail of the upper one in the band: $0<x<100$, in which only the A_n and S_n (spherical) Lamb modes are present. The coincidence frequency, x_c, occurs near the value of 20 in accordance with the rule: $x_c(h')=1$. All modes exhibit the upward turn at low frequencies due to shell curvature. The numbers along the various branches correspond to values of the mode order n, obtained from a partial-wave decomposition of the residual responses, analogous to that shown in Fig. 1, for $n=0$.

We have computed and displayed dispersion plots for the phase velocity c^p of individual Lamb waves in the shell such as A_n and S_n (cf. Figs. 5 and 6). We have generated these plots for various shell thicknesses in order to exhibit in other more conventional ways their respective frequency dependencies and their asymptotic low- and high-frequency behaviors. Although in the relatively narrow frequency bands displayed in Figs. 5 and 6, only two (spherical) Lamb modes/waves seem to be present in the shell (viz., A_n and S_n) this is not the case for broader bands. We displayed the appropriate results for a $h' = 5\%$ steel shell in water in a very broad band (viz., $0<x\leqslant 500$) in Fig. 7 to show the appearance of additional branches of the dispersion curves (viz., A_1, S_1, S_2) beyond the basic A_n and S_n ones. All these branches bear some resemblances to the analogous ones[21] for flat plates. The differences are substantial at low frequencies where the curvature effects are strongest. These effects are ignored by flat plate approaches. The phenomenon of *coincidence*[11,21] (viz., $c^p = c_1$) seems to be responsible for the region of strong flexures that develops[21] in the backscattering cross sections of shells in the neighborhood of the coincidence frequency. We note in closing that some of the poles in

the scattering amplitude of the waves returned by elastic spheres are associated with the Rayleigh wave that circumnavigates the sphere on its surface.[26] Their connection with analogous Lamb poles for shells will be studied elsewhere. For plates, their connections have been already established.[19]

ACKNOWLEDGMENT

The authors thank the IR Boards of their respective Institutions and the ONR for support.

[1]Lord Rayleigh, "On Waves Propagated Along the Plane Surface of an Elastic Solid," Proc. London Math. Soc. 17, 4–11 (1885).
[2]Lord Rayleigh. On the Free Vibrations of an infinite Plate of Homogeneous Isotropic Elastic Matter," Proc. London Math. Soc. 20, 225 (1889).
[3]H. Lamb, "On Waves in an Elastic Plate," Proc. Roy. Soc. (London) Ser. A 93, 114–128 (1916).
[4]I. Tolstoy and E. Usdin, "Wave Propagation in Elastic Plates. Low and High Mode Dispersion," J. Acoust. Soc. Am. 29, 37–42 (1957).
[5]A. Schoch, "The Reflection, Refraction and Diffraction of Sound" (in German). Ergeb. Exakten Naturwiss. 23, 127–134 (1950).
[6]F. A. Firestone, Non-Destr. Test. 7(2) (1948).
[7]H. Reissner, Helvetica Phys. Acta 11, 140–155 (1938); 11, 268 (1938).
[8]I. A. Viktorov, *Rayleigh and Lamb Waves* (Plenum, New York, 1967).
[9]L. M. Brekhovskikh, *Waves in Layered Media* (Academic, New York, 1960).
[10]M. Redwood, *Mechanical Waveguides* (Pergamon, New York, 1960).
[11]M. Ewing, W. Jardetzky, and F. Press, *Elastic Waves in Layered Media* (McGraw-Hill, New York, 1957).
[12]J. D. Achenback, *Wave Propagation in Elastic Solids* (North Holland, New York, 1973).
[13]L. Cremer, M. Heckl, and E. Ungar, *Structure-borne Sound* (Springer-Verlag, New York, 1966).
[14]B. A. Auld, *Acoustic Fields and Waves in Solids* (Wiley, New York, 1973).
[15]R. A. Phinney, "Propagation of Leaking Interface Waves," Bull. Seismol. Soc. Am. 51, 527–555 (1961).
[16]E. Strick and A. Ginzbarg, "Stonely-wave Velocities for a Fluid-solid Interface," Bull. Seismol. Soc. Am. 46, 281 (1956).
[17]R. Stoneley, "Elastic Waves at the Surface of Separation of Two Solids," Proc. Roy. Soc. (London) Ser. A 106, 416–428 (1924).
[18]J. G. Scholte, "On True and Pseudo-Rayleigh Waves," Proc. Koninkl. Ned. Akad. Wetenschap. 52, 652–653 (1949).
[19]L. Pitts, T. J. Plona, and W. G. Mayer, "Theoretical Similarities of Rayleigh and Lamb modes of Vibration," J. Acoust. Soc. Am. 60, 373–377 (1976).
[20]F. Luppé and J. Doucet, "Generation and Observation of a Stonely Wave at a Water/Metal Interface" (in French,, Acustica 64, 46–49 (1987).
[21]V. Ayres, G. Gaunaurd, C. Tsui, and M. Werby, "The Effects of Lamb Waves on the Sonar Cross-sections of Elastic Spherical Shells," Int. J. Solids Struct. 23, 937–946 (1987).
[22]M. C. Junger and D. Feit, *Sound, Structures and their Interaction* (MIT Press, Cambridge, MA, 1972).
[23]G. C. Gaunaurd, "Elastic and Acoustic Resonance Wave Scattering," Appl. Mech. Rev. 42, 143–192 (1989).
[24]D. G. Crighton, "Fluid Loading — The Interaction Between Sound and Vibration," J. Sound Vib. 133, 1–27 (1989).
[25]G. C. Gaunaurd and A. Kalnins, "Resonances in the Sonar Cross Sections of Coated Spherical Shells," Int. J. Solids Struct. 18, 1083–1102 (1982).
[26]L. Knopoff, "On Rayleigh Wave Velocities," Bull. Seismol. Soc. Am. 42, 307–308 (1952).
[27]G. C. Gaunaurd, "Techniques for Sonar Target-Identification," IEEE J. Ocean. Eng. OE-12, 419–423 (1987).